Published in final edited form as:
Biomaterials. 2011 December ; 32(35): 9415–9424. doi:10.1016/j.biomaterials.2011.08.047.

The use of injectable sonication-induced silk hydrogel for $VEGF_{165}$ and BMP-2 delivery for elevation of the maxillary sinus floor

Wenjie Zhang[1,2], **Xiuli Wang**[3,4], **Shaoyi Wang**[5], **Jun Zhao**[5], **Lianyi Xu**[1,2], **Chao Zhu**[5], **Deliang Zeng**[1,2], **Jake Chen**[6], **Zhiyuan Zhang**[5], **David L. Kaplan**[4,*], and **Xinquan Jiang**[1,2,*]

[1]Department of Prosthodontics, Ninth People's Hospital affiliated to Shanghai Jiao Tong University, School of Medicine, 639 Zhizaoju Road, Shanghai 200011, China

[2]Oral Bioengineering and regenerative medicine Lab, Shanghai Research Institute of Stomatology, Ninth People's Hospital Affiliated to Shanghai Jiao Tong University, School of Medicine, Shanghai Key Laboratory of Stomatology, 639 Zhizaoju Road, Shanghai 200011, China

[3]Dalian Institute of Chemical and physics, Chinese Academy of Sciences, Dalian 116023 China

[4]Department of Biomedical Engineering, School of Engineering, Tufts University, 4 Colby St, Medford, MA 02155, USA

[5]Department of Oral and Maxillofacial Surgery, Ninth People's Hospital, Shanghai JiaoTong University, School of Medicine, Shanghai 200011, China

[6]Division of Oral Biology, Tufts University School of Dental Medicine, One Kneeland Street, Boston, MA 02111, USA

Abstract

Sonication-induced silk hydrogels were previously prepared as an injectable bone replacement biomaterial, with a need to improve osteogenic features. Vascular endothelial growth factor ($VEGF_{165}$) and bone morphogenic protein-2 (BMP-2) are key regulators of angiogenesis and osteogenesis, respectively, during bone regeneration. Therefore, the present study aimed at evaluating in situ forming silk hydrogels as a vehicle to encapsulate dual factors for rabbit maxillary sinus floor augmentation. Sonication-induced silk hydrogels were prepared *in vitro* and the slow release of $VEGF_{165}$ and BMP-2 from these silk gels was evaluated by ELISA. For *in vivo* studies for each time point (4 and 12 weeks), 24 sinus floors elevation surgeries were made bilaterally in 12 rabbits for the following four treatment groups: silk gel (group Silk gel), silk gel/$VEGF_{165}$ (group VEGF), silk gel/BMP-2 (group BMP-2), silk gel/$VEGF_{165}$/BMP-2 (group V+B) (n=6 per group). Sequential florescent labeling and radiographic observations were used to record new bone formation and mineralization, along with histological and histomorphometric analysis. At week 4, $VEGF_{165}$ promoted more tissue infiltration into the gel and accelerated the degradation of the gel material. At this time point, the bone area in group V+B was significantly larger than

*Co-corresponding authors Ninth People's Hospital, Shanghai Jiao Tong University, School of Medicine, 639 Zhizaoju Road, Shanghai, 200011, China. Tel.: +86 21 63135412. Fax: +86 21 63136856. xinquanj@yahoo.cn, School of Engineering, Tufts University, 4 Colby St, Medford, MA 02155, USA. Tel: +1 617 627 3251. Fax: +1 617 627 3231. david.kaplan@tufts.edu.

those in the other three groups. At week 12, elevated sinus floor heights of groups BMP-2 and V+B were larger than those of the Silk gel and VEGF groups, and the V+B group had the largest new bone area among all groups. In addition, a larger blood vessel area formed in the remaining gel areas in groups VEGF and V+B. In conclusion, $VEGF_{165}$ and BMP-2 released from injectable and biodegradable silk gels promoted angiogenesis and new bone formation, with the two factors demonstrating an additive effect on bone regeneration. These results indicate that silk hydrogels can be used as an injectable vehicle to deliver multiple growth factors in a minimally invasive approach to regenerate irregular bony cavities.

1. Introduction

Osseointegrated dental implants are considered to be a useful alternative to replace missing teeth. However, patients with an edentulous posterior maxilla usually have an atrophied maxilla [1, 2]. Inadequate alveolar bone together with specific anatomic structure of maxillary sinus often hampers implant installation. Consequently, different approaches have been developed to deal with this problem, and maxillary sinus floor elevation is an effective way to restore the posterior upper jaw [3-5]. Although various bone-grafting materials, including autogenous bone, allogeneic bone and xenografts, are currently being used for maxillary augmentation, these grafts have disadvantages, including finite donor availability, potential donor site morbidity, disease transmission, immunogenic response and high cost [6-8]. As a consequence, many biomaterials with good biocompatibility have been developed as an alternative to traditional graft materials. For example, a new technology, called “injectable tissue-engineered bone”, has been a focus since the technology is minimally invasive and has good plasticity [9]. In addition, injectable tissue-engineered bone can be mixed with growth factors and cells with osteoinductive properties for irregular shaped bony cavities such as maxillary sinus floor augmentation [10-13].

Hydrogels are injectable water-swollen polymeric materials which have been used for tissue engineering and drug/growth factor release [14, 15]. Silk fibroin is a natural polymer used in the design of bioactive matrices with advantages of controlled degradability, versatile chemistry, impressive mechanical properties and low inflammatory response because of the intrinsic chemical characteristics of the protein [16-18]. Purified silk fibroin solutions can form hydrogels due to the self-assembled physical crosslinks or β-sheet crystals, under controllable conditions [19-21]. Silk hydrogels were prepared by ultrasonication in our previous studies [21]. This is a relatively simple and controllable process, as the transition time can be modulated from minutes to hours based on the sonication power and duration [21]. Previously, silk fibroin hydrogels showed compatibility with host cells and bioactive molecules [21, 22]. These advantages of silk hydrogels suggest its potential use as a carrier as a minimally invasive biomaterial for bone regeneration for irregular bony cavities. Scaffolds encapsulating individual osteogenic growth factors have demonstrated bone repair ability [23-25]. Bone regeneration involves many bioactive factors with different efficacies; the combination of VEGF and BMP-2 offers synergy towards bone regeneration [26, 27]. Angiogenesis is the first step in the tissue regeneration process and microvascular networks supply oxygen and nutrients and also facilitate cell invasion into engineered bone [28]. Among various growth factors involved in angiogenesis, $VEGF_{165}$ has been extensively investigated as a potent growth factor in driving endothelial behavior and enhancing osteogenesis. In addition, VEGF can promote osteogenesis by directing the function of osteo-related cells [29-31]. BMP-2 plays a central role in many steps during bone regeneration. During bone healing, BMP-2 stimulates both osteoblast proliferation and differentiation [32], recruits undifferentiated mesenchymal cells from peripheral tissues and facilitates precursor cell differentiation into bone-forming cells [28, 33]. BMP-2 has

demonstrated powerful *in vivo* osteogenic ability when applied locally and has been recognized as one of the most potent osteoinductive growth factors [34-37].

The objective of the present study was to assess the utility of silk hydrogels as a dual growth factor delivery vehicle for bone regeneration. $VEGF_{165}$ and BMP-2 were delivered by sonication-induced silk gels to elevate the rabbit sinus floor. Sequential observations were carried out to evaluate the effects of the silk hydrogel as a vehicle for dual growth factor delivery and for filling irregular bony cavities in the rabbit sinus.

2. Materials and Methods

2.1. Animals

A total of 24 male New Zealand rabbits with an average weight of 2.5 kg were used in this study. All animals were obtained from the Ninth People's Hospital Animal Center (Shanghai, China) and the experimental protocol was approved by the Animal Care and Experiment Committee of Ninth People's Hospital.

2.2. Silk fibroin solutions preparation

Silk fibroin stock solutions were prepared as previously described [38]. Briefly, cocoons of *Bombyx mori* were boiled in 0.02 M sodium carbonate aqueous solution for 40 min, and then rinsed thoroughly with deionized water to extract the sericin proteins. After overnight drying, the extracted silk fibroin was dissolved in 9.3 M LiBr solution at 60°C for 4 hours. Residual salt was removed by dialyzing in deionized water using Slide-a-Lyzer dialysis cassette (MWCO 3,500, Pierce) for 2 days. The final concentration of the silk fibroin was about 8.0 wt % and the 5.0 wt % solution was prepared by dilution with deionized water.

2.3. Sonication-induced gelation and growth factor capsulation

Recombinate $VEGF_{165}$ and BMP-2 protein (*gift from Wyeth*) were dissolved in deionized water and the final concentration was adjusted to 1.0 mg/ml and 1.5 mg/ml, respectively. Then 1 ml of 5.0 wt % silk fibroin solution, after autoclaving in a glass flask, was sonicated at 25% amplitude for 30 s. Four study groups of silk gel were prepared: (1) silk gel alone (Silk gel); (2) silk gel encapsulated with $VEGF_{165}$ (VEGF); (3) silk gel encapsulated with BMP-2 (BMP-2); (4) silk gel encapsulated with $VEGF_{165}$ and BMP-2 (V+B). For different experimental groups, the mixture of 20 μl $VEGF_{165}$ solution and 20 μl deionized water, the mixture of 20 μl BMP-2 solution and 20 μl deionized water, or the mixture of 20 μl $VEGF_{165}$ and 20 μl BMP-2 was added to the sonicated silk solution immediately and mixed gently. Then 40 μl deionized water was added in the control gel alone group. The mixed solutions were aspirated in 1 ml syringes and placed in 37°C for 1~6 hours to allow gelation (Fig. 1a-c). All the operations were carried out in the laminar flow cabinet.

2.4. Release kinetics of $VEGF_{165}$ and BMP-2 from silk gels *in vitro*

After undergoing the self-assembly transition to the gel state in the 1 ml syringe, silk hydrogel with encapsulated $VEGF_{165}$ and BMP-2 was cut into 0.5 cm long cylinder-shape segments (about 100 μl). These segments were washed three times with 1×PBS before being placed in a microcentrifuge tube containing 1 ml 1×PBS and incubated at 37°C. At each selected time point (1, 3, 7, 14, 28 days), the supernatant was collected and stored at -80°C. The gels were resuspended in fresh PBS and incubated until the next time point. The release of $VEGF_{165}$ and BMP-2 was quantified using ELISA kits (Becton, Dickinson & Company, USA), respectively, according to the manufacturers' instructions [10].

2.5. Maxillary sinus floor elevation procedure

The observation time points in this study were set at week 4 and week 12. A total of 24 rabbits were randomly allocated into 4 study groups. Each group included 3 animals with 6 maxillary sinuses (n=6) at both time points. After general anesthesia through the intramuscular injection of ketamine (40 mg/kg), the sinus floor elevation surgery was performed as our previously described methods [39]. Briefly, a 2.5 cm midline incision was made on the nasal dorsum, and the skin and periosteum were lifted to expose the nasal bone and nasoincisal suture line. Two round bone windows (diameter, about 0.4 cm) located approximately 2 cm anterior to the nasofrontal suture line, 0.5 cm lateral to the midline were opened, using a round bur, in the nasal bone bilaterally. Care was taken to protect the sinus mucosa. A freer elevator was used to peel and push the mucosa inward gently, and 200 μl of each silk gel was injected into the elevated cavity from the syringe separately for each group (Fig. 1d). The elevated height was defined as the maximal distance between sinus bony floors and raised nasal dorsum in the augmented space (Fig. 1e).

2.6. Radiographic observation

Radiographic images were obtained immediately and at 4, 8 and 12 weeks after maxillary sinus floor elevation surgery. Lateral jaw radiographies were obtained under anesthesia with a dental X-ray machine (Trophy, France), from a distance of 5 cm with an exposure time of 0.28 s (280 V, 8 mA), to follow new bone formation and mineralization.

2.7. Sequential fluorescent labeling

A polychrome sequential fluorescent labeling method was carried out on rabbits sacrificed at week 12 to observe the rate of new bone formation and mineralization, as previously described [40]. For this assay 25 mg/kg tetracycline hydrochloride (TE, Sigma, USA), 20 mg/kg calcein (CA, Sigma, USA) and 30 mg/kg alizarin red S (AL, Sigma, USA) were administrated intraperitoneally at 3, 6 and 9 weeks after surgery, respectively.

2.8. Sample preparation

The rabbits sacrificed at 4 weeks were exsanguinated via jugular vein and perfused via bilateral carotid arteries with 10% buffered formaldehyde (pH 7.4) as we have previously described [39]. The maxillae were dissected along the midline and trimmed into smaller blocks, and then fixed in the same 10% buffered formaldehyde solution. Rabbits from the week 12 observation groups were perfused with Microfil (Flow Tech, USA) via bilateral carotid arteries. First, 200 ml heparinized saline was used to clear the blood existing in the craniofacial vessels. The blue colored Microfil solution was subsequently infused at a slow rate of 5 ml/min until the whole tongue was clearly colored blue. The samples were then allowed to polymerize over two hours before small blocks were trimmed and fixed in 10% buffered formaldehyde solution.

2.9. Micro-Computed tomography scanning

The fixed samples at 12 weeks were imaged with a desktop Micro-CT system (μCT-80, Scanco Medical, Switzerland) in high-resolution scanning mode (pixel matrix, 1024×1024; voxel size, 20 μm; slice thickness, 20 μm) to determine bone volume. To obtain the original three dimensional (3D) image, a threshold value of 225 was chosen to segment the Micro-CT images for all specimens using the analyze software package (Scanco Medical, Switzerland). The 3D reconstructed images were presented to show new bone formation in the elevated sinus area by cutting the buccal and lingual into two halves. Bone mineral density (BMD), bone volume fraction (Bone volume/total volume, BV/TV), and trabecular thickness of new bone were analyzed as previously described [7].

2.10. Histological and histomorphometric observations

The elevated sinuses of rabbits sacrificed at week 12 were bisected along the sagittal plane of the mesiodiatal direction and cut into the buccal and lingual halves along the top of the maxillary sinus. The height of augmented maxillary sinus floor was measured on these longitudinal sections as shown in Figure 1 (e). One half of the sample was decalcified, embedded in paraffin and sectioned into 4 μm thick sections. Three randomly selected sections were stained with hematoxylin-eosin (HE). The other half was dehydrated, embedded in polymethylmethacrylate (PMMA) and cut into 150 μm thick sections using a microtome (Leica, Germany). These sections were gradually ground and polished to a thickness of 40 μm [41]. All samples of the week 4 observation group were decalcified and stained with HE as above. Decalcified specimens were subjected to histological and histomorphometric observations and analyzed using a personal computer-based system (Image-Pro Plus™, USA). Nondecalcified sections were observed for fluorescent labeling under confocal laser scanning microscope (CLSM, Leica, Germany). Excitation/emission wavelengths of chelating fluorochromes were used 405/580 nm, 488/517 nm and 543/617 nm for TE (yellow), CA (green) and AL (red), respectively. As shown in Fig. 4b, rectangle regions (100x magnification) located in the center of the elevated sinus membrane margin along the maximal sagittal plane were used to quantify the different fluorescently labelled areas to reflect the ingrowth of new bone. All images were stored digitally and the histomorphometric observations were analyzed using Image-Pro Plus™ software [40]. The numbers of TE, CA and AL labeled pixels in each image represent bone regeneration and mineralization at 3, 6 and 9 weeks after operation. The undecalcified sections were further stained with Von Gieson's picro fuchsin [42]. The percentage of blue colored Microfil areas on these sections was calculated with Image-Pro Plus™ software to evaluate blood vessel formation in each group.

2.11. Statistical analysis

All the data were expressed as mean ± standard deviation. Statistically significant differences ($p < 0.05$) among the various groups were measured using ANOVA and SNK post hoc based on the normal distribution and equal variance assumption test. All statistical analysis was carried out using an SAS 8.2 statistical software package (Cary, USA).

3. Results

3.1. Gross observation

The injectable property of silk gels makes them relatively easy to utilize when used to lift the sinus floor, with smaller bone windows compared to previous animal models for the insertion of blocks for filling. All animals were given antibiotics through intramuscular injection 3 days after the operation and therefore were only slight soft tissue edema in a few rabbits that disappeared 2-4 days post-operation. No infections were detected within the 4 or 12 week observation periods.

3.2. The release of $VEGF_{165}$ and BMP-2 from silk gel

The $VEGF_{165}$ and BMP-2 ELISA kits were used to quantify the release of growth factors from silk gels. Figure 2 reflects the cumulative release of the two growth factors when incubated *in vitro*. There was no obvious burst release for both growth factors after the initial *in vitro* culture. After one day, the release of $VEGF_{165}$ and BMP-2 was 12,659 ± 1,867 pg/ml and 16,677 ± 1,828 pg/ml, respectively. $VEGF_{165}$ and BMP-2 were slowly released from the dual factor encapsulated silk gels and after 14 days the release kinetics showed a cumulative release of $VEGF_{165}$ and BMP-2 with 43,891 ± 6,262 pg/ml and 60,952 ± 4,459 pg/ml, respectively. Over a 28 days period the cumulative release was 62,909 ±

7,836 pg/ml for $VEGF_{165}$ and 87,423 ± 6,205 pg/ml for BMP-2. Therefore, fabricating silk gels as a vehicle to deliver growth factors provided sustained release kinetics.

3.3. Radiographic examination

To trace new bone formation, sequential radiographic images of each study group were obtained (Fig.3). Immediately after the operation, all sinus lifting areas were radiolucent. No obvious difference could be detected among the four groups. From visual inspection, the Silk gel group changed little at 12 weeks post operation. In the VEGF group, a slight radiopaque area was able to be told at 8 weeks after the operation, and at 12 weeks, there was a small shadow on the top of sinus lifting area. In the BMP-2 group, the radiographic bone density was higher from 4 weeks and the opaque area was larger than that in the VEGF group at 12 weeks. In the V+B group, the opaque image could be distinguished as early as 4 weeks after operation. Also, the radiographic bone density was relatively higher than that in group BMP-2 at 8 and 12 weeks, respectively.

3.4. Sequential fluorescent labeling histomorphometrical analysis

In order to avoid the probable interference from fluorescent labeling by remineralization and remolding of marginal autogenous bone tissue (such as sinus bony floors and nasal dorsum), the regions adjacent to the elevated sinus membrane margin were chosen to quantify the different fluorescences labelled areas to reflect the ingrowth of new bone. The process of new bone formation and mineralization was recorded by measuring the areas of TE, CA, AL flurochome stained bone. From the images of Fig. 4a, fluorescent labeling areas of group BMP-2 and group V+B were more strongly fluorescent than that of the other two groups at all stages. Figure 4c displays the histomorphometrical analysis results, at 3 weeks post-operation, the percentage of TE labeled area (yellow) in group V+B was 2.06 ± 0.28%, which was higher than the VEGF group (0.28 ± 0.09%), the Silk gel group (0.02 ± 0.01%) or the BMP-2 group (1.41 ± 0.16%) ($p < 0.05$). At 6 weeks post-operation, the percentage of CA labeled area (green) in the BMP-2 group was 1.87 ± 0.38% and group V+B was 2.18 ± 0.28%, which were higher than in the Silk gel group (0.25 ± 0.06%) or VEGF group (0.38 ± 0.09%) ($p < 0.05$). At 9 weeks post-operation, the percentage of AL labeled area (red) was 0.50 ± 0.13%, 0.97 ± 0.27%, 2.01 ± 0.33% and 2.50 ± 0.36% for the Silk gel, VEGF, BMP-2 and V+B groups, respectively. There were significant differences between the V+B group and other three groups ($p < 0.05$). Taking all of the data into consideration, more newly formed bone infiltrated into the gels in group V+B, with $VEGF_{165}$ additively promoting new bone formation even from the initial stages. Neoformative bone mass was increased when compared to BMP-2 alone.

3.5. Histological findings of new bone formation

At 4 weeks after implantation, there was little new bone formation in the Silk gel group. The whole sinus was still almost filled with gel and the percentage of new bone area among the augmented area was only 1.75 ± 0.34%. Group V+B demonstrated significant new bone formation (30.22 ± 2.91%) that was significantly higher than that of the BMP-2 (17.12 ± 3.40%) and VEGF (5.57 ± 1.30%) ($p < 0.05$) groups. In group V+B and group VEGF, the percent of remnant gel area of these two groups was 50.97 ± 8.58% and 50.24 ± 7.40%, respectively, which were less than that of the BMP-2 group (64.01 ± 4.98%) and Silk gel group (73.93 ± 4.40%) (Figs. 5, 6) ($p < 0.05$).

Compared with 4 weeks, newly formed bone in all four groups increased at 12 weeks. The percentage of new bone area in group V+B was 42.45 ± 4.93%, which was significantly higher than that of group BMP-2 (32.97 ± 5.53%), group VEGF (18.52 ± 5.64%) and the Silk gel group (8.70 ± 2.92%) ($p < 0.05$). The silk gel degraded faster in group V+B and group VEGF. The percentage of remnant gel area in group V+B and group VEGF at 12

weeks were 30.14 ± 5.95% and 32.13 ± 5.64%, respectively, which were less than that of group BMP-2 (40.22 ± 6.23%) and group Silk gel (52.81 ± 5.51%) ($p < 0.05$) (Fig. 5 and Fig. 6).

3.6. Micro-CT measurements

The morphology of the newly formed bone in the week 12 samples was reconstructed (Fig. 5). No obvious bone formation was observed in group Silk gel (i). While in group VEGF (j), a thin layer of trabecular bone protruded into the sinus from the surrounding bony wall and elevated membrane. More new bone invading into the sinus was observed in group BMP-2 (k). By comparison, in group V+B (l), the volume of newly formed bone protruding into the sinus was further increased. Results of quantitative analysis are shown in Fig. 6. Bone mineral density (BMD) and the ratio of bone volume to total volume (BV/TV) were significantly higher for group V+B when compared to the other three groups ($p < 0.05$). In addition, the trabecular thickness (Tb.Th) and trabecular number (Tb.N) for the V+B group were also higher than the other three groups ($p < 0.05$).

3.7 Neo-angiogenesis in the sinus

We further investigated the effect of $VEGF_{165}$ on neo-angiogenesis of the elevated sinus area. As shown in Fig. 7, red areas represent newly formed bone on the nondecalcified sections. The blue colored Microfil labeled area was calculated to reflect the vascularization of newly formed bone. The percent of new blood vessel area in group VEGF and group V+B were 4.66 ± 0.97% and 4.98 ± 1.01%, respectively, which was significantly higher than that of group Silk gel or group BMP-2 ($p < 0.05$).

3.8. The elevated height analysis

The height of the elevated sinus floor at 12 weeks was measured to assess the sinus augmentation effects of the different silk hydrogel complexes. The elevated height of group BMP-2 was 11.45 ± 0.69 mm and group V+B was 11.53 ± 0.78 mm (Fig. 8). There was no significant difference between group BMP-2 and group V+B. But the elevated heights of these two groups were all higher than that of group VEGF (8.52 ± 0.67 mm) or group Silk gel (7.52 ± 0.82 mm) ($p < 0.05$).

3.9 Degradation of silk gel

Following tissue ingrowth into the silk gels, a line of osteoblasts was observed around newly formed bone (Fig. 9a). In addition, similarly to previous degradation of silk fiber and scaffold [43, 44], multinucleated giant cells was also visible adjacent to the residual silk gel which was close to the newly formed bones at week 4 (Fig. 9b). Those giant cells may participate in the degradation of silk gel. Silk gel fragments engulfing by multinucleated giant cells were shown in Fig. 9c. At week 12, more giant cells were detected around degrading silk gel as tissue ingrowth occurred gradually (Fig. 9d).

4. Discussion

Maxillary sinus floor augmentation has been widely used as a surgical procedure to gain bone mass for placement of dental implants. The elevated space demands sufficient bone graft material filling to obtain adequate bone support. In the present study, a rabbit model was used which has been well documented for sinus reconstruction. The maxillary sinus of the rabbit has a well-defined ostium similar to that in humans [45]. When the sinus membrane was elevated, an irregular cavity is formed. The injectable silk gel could be beneficial in such applications since it is easy to manipulate to fill the irregular bony cavity, which may shorten the surgical operation time and minimize surgical damage.

Sonication-induced silk hydrogels were used for dual growth factor delivery to elevate the rabbit sinus floor. After sonication, the growth factors were added to the silk solution and the sol-gel transition process was completed within several hours. The silk fibroin hydrogel as a delivery system is simple and convenient for preparation and clinical applications and pending conditions of sonication the process can be shorted to minutes if needed [21]. Although the use of a silk gel alone did not promote sufficient new bone formation in the rabbit model, it could serve as a useful vehicle to deliver bioactive growth factors. Angiogenic and osteogenic factors released from silk gel promoted tissue invasion and new bone formation. More importantly, our *in vitro* studies confirmed that $VEGF_{165}$ and BMP-2 exhibited sustained release but not burst release, from the silk fibroin hydrogels. Thus, with further optimization it should be possible to control the release process by adjusting growth factor loading and gel biodegradation rate [44, 46]. In addition, the quality of protein released from a sustained delivery matrix is of critical importance for substantial bone regeneration. In our recent studies [46], we demonstrated that functional stability and released bioactive factors from silk fibroin hydrogels were comparable to that of unincorporated bioactive protein controls, which indicates that the incorporation in silk fibroin hydrogels does not affect bioactivity.

Maxillary sinus augmentation, as a bone regeneration procedure, also involves various bioactive factors [47, 48]. In this study, encapsulating growth factors increased the ability of the silk gel to mediate bone regeneration in the augmented sinus region of the rabbit. In particular, the combination of $VEGF_{165}$ and BMP-2 resulted in enhanced osteogenesis over $VEGF_{165}$ or BMP-2 alone. According to the sequential radiographic results, opaque areas were detected as early as four weeks after implantation in the V+B group, while higher radiographic bone density was detected after 8 weeks after implantation in the BMP-2 group. In addition, polychrome sequential fluorescent labeling was used to record new bone deposition and the mineralization process. Fluorescent TE was administered intraperitoneally 3 weeks after the operation. The percentage of TE labeling area was significantly higher than that of the BMP-2 group. These findings showed that the combination of $VEGF_{165}$ and BMP-2 promoted new bone formation even at initial stages of the repair process.

As previously mentioned, $VEGF_{165}$ and BMP-2 can bring additive effects. $VEGF_{165}$ as a powerful angiogenic factor promotes angiogenesis and vasculogenesis, which are important for tissue development and regeneration. But the delivery of a single angiogenic agent was not sufficient for bone regeneration, as shown in this study. However, $VEGF_{165}$ was able to enhance the effect of bone formation induced by BMP-2 alone. Most likely, the additive effect was mainly brought about by contributing to the angiogenic response, which is supported by previous studies [28, 49]. After the construction of a vascular network, the amounts of mesenchymal stem cells or osteoprogenitor cells would be transported by circulation, and the sustained release of BMP-2 further induced those cells into the osteogenic lineage. In addition, $VEGF_{165}$ would also directly promote osteogenesis by affecting osteoblasts as well as enhancing osteogenic differentiation of mesenchymal stem cells [29-31]. These direct and indirect effects of $VEGF_{165}$ not only promote early new bone formation but also enhance the quality of newly formed bone.

The current study revealed that the remnants of silk gel in the VEGF and V+B groups were less than that of the other two groups. $VEGF_{165}$ accelerated new tissue ingrowth by promoting new blood vessel formation and this process increased the interface between autologous tissue and the silk gel, which may accelerate silk gel degradation. In our previous study [44], the immune system played a significant role in the degradation of silk scaffolds. Macrophages and multinucleated giant cells quickly invaded and concentrated around silk scaffold pieces as tissue ingrowth took place. Cell-mediated degradation of silk gels was

also detected in our study. At week 4, multinucleated giant cells were observed concentrating around silk gel pieces at the interface between tissue and gel. As tissue ingrowth gradually increased, more giant cells participated in silk gel degradation, resulting in more space for tissue ingrowth.

Based on the above results, dual $VEGF_{165}$ and BMP-2 delivery could be encapsulated into the silk gel, and the injectable delivery system achieved beneficial effects in the rabbit sinus floor elevation model. The released biological factors promoted angiogenesis, tissue ingrowth and bone regeneration. Since the silk gel alone lacks internal pores for initial tissue ingrowth, the fabrication of the silk gel with improved porous structure may enhance its use as a bone-grafting biomaterial.

5. Conclusions

Sonication-induced silk hydrogels served as useful vehicles to encapsulate and slowly release of $VEGF_{165}$ and BMP-2. For the irregular shaped rabbit sinus model, the use of the silk gel had many advantages including good plasticity, minimal invasion and short utility at operation time. The combination of angiogenic and osteogenic growth factors brought about additive effects on bone formation. Dual factor encapsulated silk gels promoted bone regeneration as well as maintained the augmented height in the rabbit sinus floor elevation model. These results offer a potential alternative bone-grafting material for edentulous maxillary sinus floor augmentation and the repair of other bony cavities in the clinic.

Acknowledgments

The authors appreciate Carmen Preda for the preparation of the silk solutions for the study. This work was supported by National Natural Science Foundation of China 30772431, 30973342. Science and Technology Commission of Shanghai Municipality 08410706400, 0952nm04000, 10dz2211600. Program for New Century Excellent Talents in University NCET-08-0353. Shanghai Education Committee 07SG19. We also thank the NIH (DK) [DE017207, EB003210, EB002520, DE16710 and DE21464] for support of these studies.

References

1. Boyne PJ, Lilly LC, Marx RE, Moy PK, Nevins M, Spagnoli DB, et al. De novo bone induction by recombinant human bone morphogenetic protein-2 (rhBMP-2) in maxillary sinus floor augmentation. J Oral Maxillofac Surg. 2005; 63:1693–707. [PubMed: 16297689]
2. Hirsch J, Ericsson I. Maxillary sinus augmentation using mandibular bone grafts and simultaneous installation of implants. A surgical technique. Clin Oral Implants Res. 1991; 2:91–6. [PubMed: 1809404]
3. Vlassis JM, Hurzeler MB, Quinones CR. Sinus lift augmentation to facilitate placement of nonsubmerged implants: a clinical and histological report. Pract Periodontics Aesthet Dent. 1993; 5:15–23. quiz 24. [PubMed: 8400221]
4. Derong Z, Lian G, Jiayu L, Xiuli Z, Zhiyuan Z, Xinquan J. Anatomic and histological analysis in a goat model used for maxillary sinus floor augmentation with simultaneous implant placement. Clin Oral Implants Res. 2010; 21:65–70. [PubMed: 20070749]
5. Jiang XQ, Sun XJ, Lai HC, Zhao J, Wang SY, Zhang ZY. Maxillary sinus floor elevation using a tissue-engineered bone complex with beta-TCP and BMP-2 gene-modified bMSCs in rabbits. Clin Oral Implants Res. 2009; 20:1333–40. [PubMed: 19709061]
6. Damien CJ, Parsons JR. Bone graft and bone graft substitutes: a review of current technology and applications. J Appl Biomater. 1991; 2:187–208. [PubMed: 10149083]
7. Jiang X, Zhao J, Wang S, Sun X, Zhang X, Chen J, et al. Mandibular repair in rats with premineralized silk scaffolds and BMP-2-modified bMSCs. Biomaterials. 2009; 30:4522–32. [PubMed: 19501905]
8. Mangano C, Piattelli A, Mangano A, Mangano F, Mangano A, Iezzi G, et al. Combining scaffolds and osteogenic cells in regenerative bone surgery: a preliminary histological report in human

maxillary sinus augmentation. Clin Implant Dent Relat Res. 2009; 11(Suppl 1):e92–102. [PubMed: 19673958]

9. Yamada Y, Nakamura S, Ito K, Kohgo T, Hibi H, Nagasaka T, et al. Injectable tissue-engineered bone using autogenous bone marrow-derived stromal cells for maxillary sinus augmentation: clinical application report from a 2-6-year follow-up. Tissue Eng Part A. 2008; 14:1699–707. [PubMed: 18823276]
10. Kanczler JM, Ginty PJ, White L, Clarke NM, Howdle SM, Shakesheff KM, et al. The effect of the delivery of vascular endothelial growth factor and bone morphogenic protein-2 to osteoprogenitor cell populations on bone formation. Biomaterials. 2010; 31:1242–50. [PubMed: 19926128]
11. Velich N, Németh Z, Tóth C, Szabó G. Long-term results with different bone substitutes used for sinus floor elevation. J Craniofac Surg. 2004; 15:38–41. [PubMed: 14704560]
12. Zhou Y, Ni Y, Liu Y, Zeng B, Xu Y, Ge W. The role of simvastatin in the osteogenesis of injectable tissue-engineered bone based on human adipose-derived stromal cells and platelet-rich plasma. Biomaterials. 2010; 31:5325–35. [PubMed: 20381859]
13. Aral A, Yalçin S, Karabuda ZC, Anil A, Jansen JA, Mutlu Z. Injectable calcium phosphate cement as a graft material for maxillary sinus augmentation: an experimental pilot study. Clin Oral Implants Res. 2008; 19:612–7. [PubMed: 18474064]
14. Lee KY, Mooney DJ. Hydrogels for tissue engineering. Chem Rev. 2001; 101:1869–79. [PubMed: 11710233]
15. Langer R. Biomaterials in drug delivery and tissue engineering: one laboratory's experience. Acc Chem Res. 2000; 33:94–101. [PubMed: 10673317]
16. Silva SS, Motta A, Rodrigues MT, Pinheiro AF, Gomes ME, Mano JF, et al. Novel genipin-cross-linked chitosan/silk fibroin sponges for cartilage engineering strategies. Biomacromolecules. 2008; 9:2764–74. [PubMed: 18816100]
17. Gil ES, Frankowski DJ, Spontak RJ, Hudson SM. Swelling behavior and morphological evolution of mixed gelatin/silk fibroin hydrogels. Biomacromolecules. 2005; 6:3079–87. [PubMed: 16283730]
18. Zhao J, Zhang Z, Wang S, Sun X, Zhang X, Chen J, et al. Apatite-coated silk fibroin scaffolds to healing mandibular border defects in canines. Bone. 2009; 45:517–27. [PubMed: 19505603]
19. Yucel T, Cebe P, Kaplan DL. Vortex-induced injectable silk fibroin hydrogels. Biophys J. 2009; 97:2044–50. [PubMed: 19804736]
20. Kim UJ, Park J, Li C, Jin HJ, Valluzzi R, Kaplan DL. Structure and properties of silk hydrogels. Biomacromolecules. 2004; 5:786–92. [PubMed: 15132662]
21. Wang X, Kluge JA, Leisk GG, Kaplan DL. Sonication-induced gelation of silk fibroin for cell encapsulation. Biomaterials. 2008; 29:1054–64. [PubMed: 18031805]
22. Lutolf MP, Hubbell JA. Synthetic biomaterials as instructive extracellular microenvironments for morphogenesis in tissue engineering. Nat Biotechnol. 2005; 23:47–55. [PubMed: 15637621]
23. Li M, Liu X, Ge B. Calcium phosphate cement with BMP-2-loaded gelatin microspheres enhances bone healing in osteoporosis: a pilot study. Clin Orthop Relat Res. 2010; 468:1978–85. [PubMed: 20306162]
24. Gutwald R, Haberstroh J, Stricker A, Rüther E, Otto F, Xavier SP, et al. Influence of rhBMP-2 on bone formation and osseointegration in different implant systems after sinus-floor elevation. An *in vivo* study on sheep. J Craniomaxillofac Surg. 2010; 38:571–9. [PubMed: 20381369]
25. Bessa PC, Balmayor ER, Hartinger J, Zanoni G, Dopler D, Meinl A, et al. Silk fibroin microparticles as carriers for delivery of human recombinant bone morphogenetic protein-2: *in vitro* and *in vivo* bioactivity. Tissue Eng Part C Methods. 2010; 16:937–45. [PubMed: 19958078]
26. Samee M, Kasugai S, Kondo H, Ohya K, Shimokawa H, Kuroda S. Bone morphogenetic protein-2 (BMP-2) and vascular endothelial growth factor (VEGF) transfection to human periosteal cells enhances osteoblast differentiation and bone formation. J Pharmacol Sci. 2008; 108:18–31. [PubMed: 18776714]
27. Peng H, Usas A, Olshanski A, Ho AM, Gearhart B, Cooper GM, et al. VEGF improves, whereas sFlt1 inhibits, BMP2-induced bone formation and bone healing through modulation of angiogenesis. J Bone Miner Res. 2005; 20:2017–27. [PubMed: 16234975]

28. Kempen DH, Lu L, Heijink A, Hefferan TE, Creemers LB, Maran A, et al. Effect of local sequential VEGF and BMP-2 delivery on ectopic and orthotopic bone regeneration. Biomaterials. 2009; 30:2816–25. [PubMed: 19232714]
29. Street J, Bao M, deGuzman L, Bunting S, Peale FV Jr, Ferrara N, et al. Vascular endothelial growth factor stimulates bone repair by promoting angiogenesis and bone turnover. Proc Natl Acad Sci U S A. 2002; 99:9656–61. [PubMed: 12118119]
30. Behr B, Tang C, Germann G, Longaker MT, Quarto N. Locally applied ascular endothelial growth factor a increases the osteogenic healing capacity of human adipose-derived stem cells by promoting osteogenic and endothelial differentiation. Stem Cells. 2011; 29:286–96. [PubMed: 21732486]
31. Geiger F, Bertram H, Berger I, Lorenz H, Wall O, Eckhardt C, et al. Vascular endothelial growth factor gene-activated matrix (VEGF165-GAM) enhances osteogenesis and angiogenesis in large segmental bone defects. J Bone Miner Res. 2005; 20:2028–35. [PubMed: 16234976]
32. Rath B, Nam J, Knobloch TJ, Lannutti JJ, Agarwal S. Compressive forces induce osteogenic gene expression in calvarial osteoblasts. J Biomech. 2008; 41:1095–103. [PubMed: 18191137]
33. Zhao J, Hu J, Wang S, Sun X, Xia L, Zhang X, et al. Combination of beta-TCP and BMP-2 gene-modified bMSCs to heal critical size mandibular defects in rats. Oral Dis. 2010; 16:46–54. [PubMed: 19619194]
34. Chen B, Lin H, Wang J, Zhao Y, Wang B, Zhao W, et al. Homogeneous osteogenesis and bone regeneration by demineralized bone matrix loading with collagen-targeting bone morphogenetic protein-2. Biomaterials. 2007; 28:1027–35. [PubMed: 17095085]
35. Schliephake H, Weich HA, Dullin C, Gruber R, Frahse S. Mandibular bone repair by implantation of rhBMP-2 in a slow release carrier of polylactic acid--an experimental study in rats. Biomaterials. 2008; 29:103–10. [PubMed: 17936352]
36. Zhou M, Peng X, Mao C, Xu F, Hu M, Yu GY. Primate mandibular reconstruction with prefabricated, vascularized tissue-engineered bone flaps and recombinant human bone morphogenetic protein-2 implanted in situ. Biomaterials. 2010; 31:4935–43. [PubMed: 20346504]
37. Chen D, Zhao M, Mundy GR. Bone morphogenetic proteins. Growth Factors. 2004; 22:233–41. [PubMed: 15621726]
38. Sofia S, McCarthy MB, Gronowicz G, Kaplan DL. Functionalized silk-based biomaterials for bone formation. J Biomed Mater Res. 2001; 54:139–48. [PubMed: 11077413]
39. Sun XJ, Zhang ZY, Wang SY, Gittens SA, Jiang XQ, Chou LL. Maxillary sinus floor elevation using a tissue-engineered bone complex with OsteoBone and bMSCs in rabbits. Clin Oral Implants Res. 2008; 19:804–13. [PubMed: 18705812]
40. Wang S, Zhang Z, Zhao J, Zhang X, Sun X, Xia L, et al. Vertical alveolar ridge augmentation with beta-tricalcium phosphate and autologous osteoblasts in canine mandible. Biomaterials. 2009; 30:2489–98. [PubMed: 19147220]
41. Wang S, Zhang Z, Xia L, Zhao J, Sun X, Zhang X, et al. Systematic evaluation of a tissue-engineered bone for maxillary sinus augmentation in large animal canine model. Bone. 2010; 46:91–100. [PubMed: 19761881]
42. Wang S, Zhang W, Zhao J, Ye D, Zhu C, Yang Y, et al. Long-term outcome of cryopreserved bone-derived osteoblasts for bone regeneration *in vivo*. Biomaterials. 2011; 32:4546–55. [PubMed: 21459433]
43. Panilaitis B, Altman GH, Chen J, Jin HJ, Karageorgiou V, Kaplan DL. Macrophage responses to silk. Biomaterials. 2003; 24:3079–85. [PubMed: 12895580]
44. Wang Y, Rudym DD, Walsh A, Abrahamsen L, Kim HJ, Kim HS, et al. *In vivo* degradation of three-dimensional silk fibroin scaffolds. Biomaterials. 2008; 29:3415–28. [PubMed: 18502501]
45. Kumlien J, Schiratzki H. The vascular arrangement of the sinus mucosa. A study in rabbits. Acta Otolaryngol. 1985; 99:122–32. [PubMed: 3976385]
46. Guziewicz N, Best A, Perez-Ramirez B, Kaplan DL. Lyophilized silk fibroin hydrogels for the sustained local delivery of therapeutic monoclonal antibodies. Biomaterials. 2011; 32:2642–50. [PubMed: 21216004]

47. Boëck-Neto RJ, Artese L, Piattelli A, Shibli JA, Perrotti V, Piccirilli M, et al. VEGF and MVD expression in sinus augmentation with autologous bone and several graft materials. Oral Dis. 2009; 15:148–54. [PubMed: 19036054]

48. Degidi M, Artese L, Rubini C, Perrotti V, Iezzi G, Piattelli A. Microvessel density and vascular endothelial growth factor expression in sinus augmentation using Bio-Oss. Oral Dis. 2006; 12:469–75. [PubMed: 16910917]

49. Hansen-Algenstaedt N, Joscheck C, Wolfram L, Schaefer C, Müller I, Böttcher A, et al. Sequential changes in vessel formation and micro-vascular function during bone repair. Acta Orthop. 2006; 77:429–39. [PubMed: 16819682]

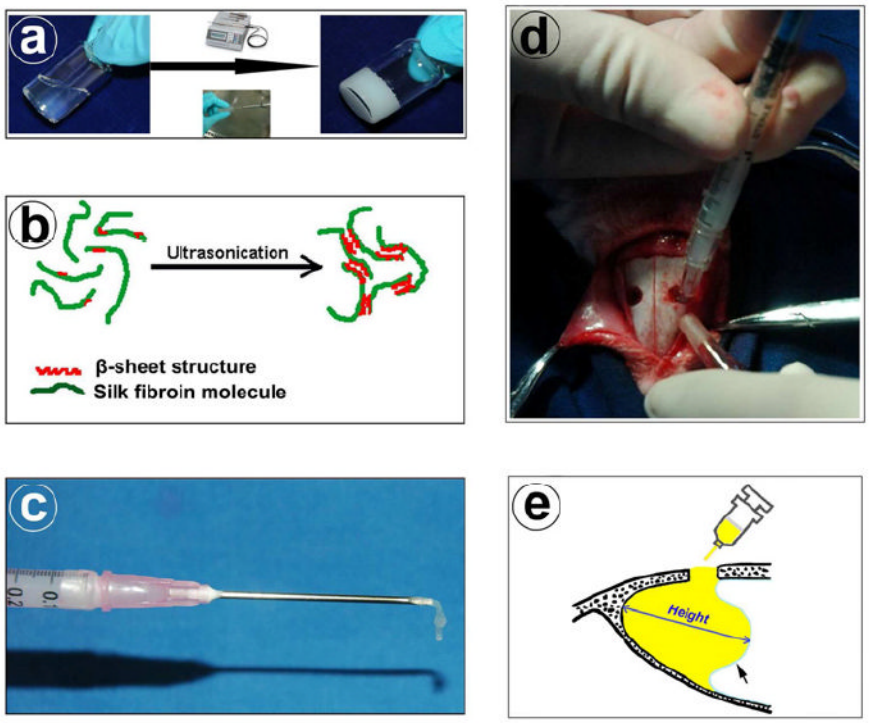

Fig. 1.

Silk hydrogel preparation and rabbit sinus floor elevation surgery: (a) Liquid phase silk solution transforms into solid silk hydrogel by ultrasonication. (b) Schematic illustration of the mechanism of silk sol-gel transition due to inter-chain physical crosslinked β-sheet structures formed after ultrasonication. (c) Injectable property of silk gel. (d) Silk gel being injected into the rabbit sinus from the small bony window. (e) Diagram of elevated sinus in sagittal plane section. Yellow area represents silk gel in the sinus cavity. The maximal distance between sinus bony floor and raised nasal dorsum is defined as the augmented height of sinus (arrow = elevated sinus mucosa).

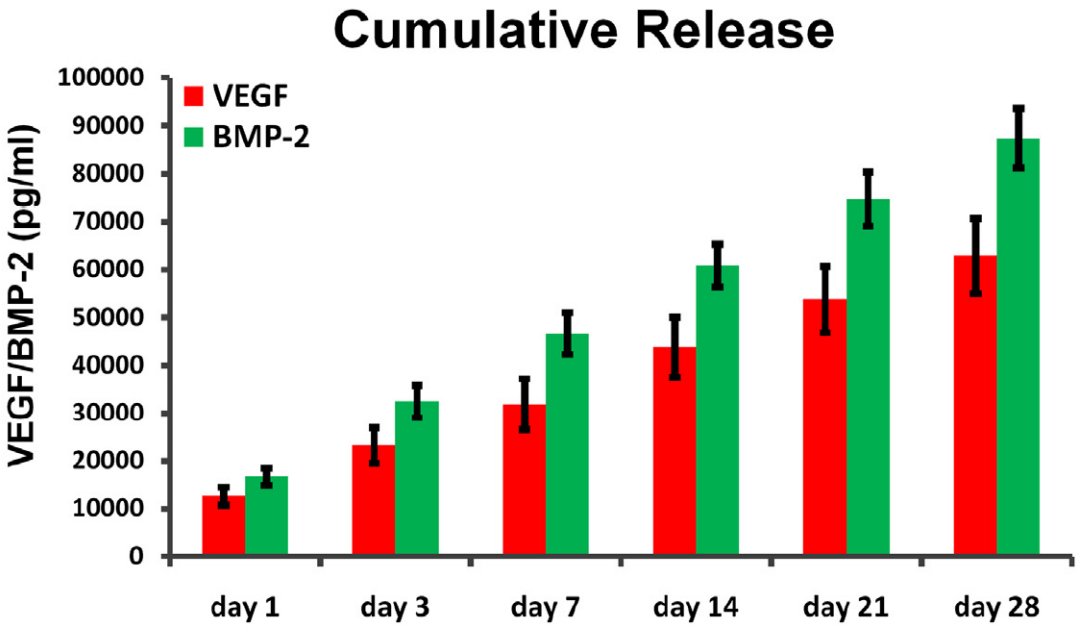

Fig. 2.
Cumulative release of $VEGF_{165}$ and BMP-2 from silk gels detected by ELISA.

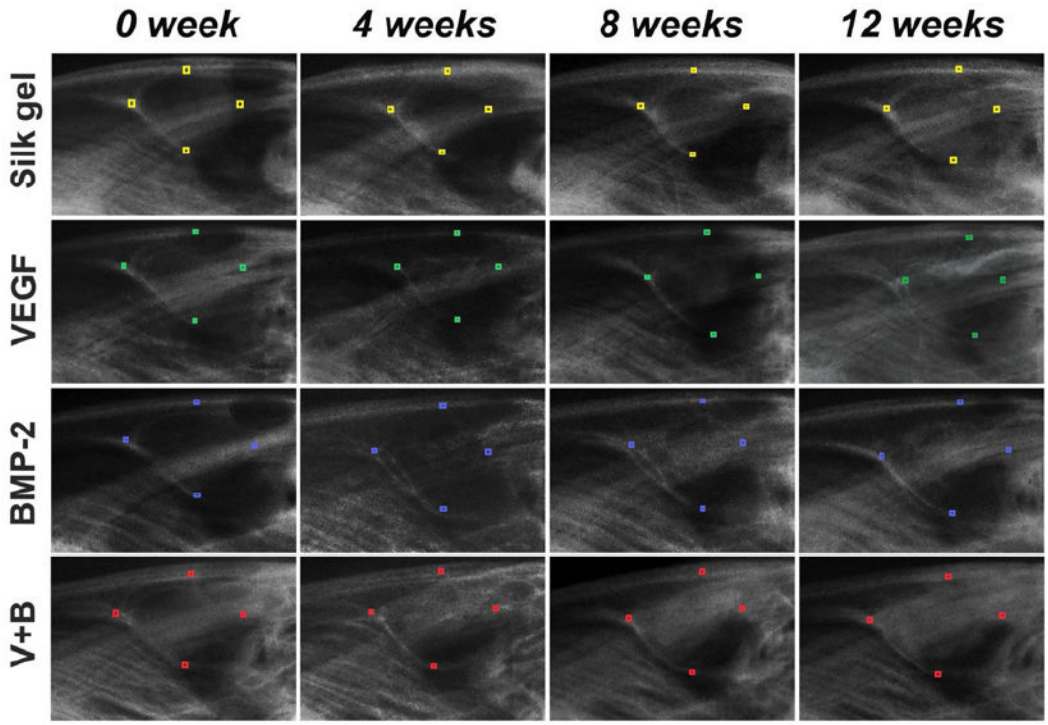

Fig. 3.

Sequential radiographic observation immediately, 4 weeks, 8 weeks and 12 weeks post-operation. The front-end, back-end, apex and lowest point of the four different groups are marked with different colored small rectangles.

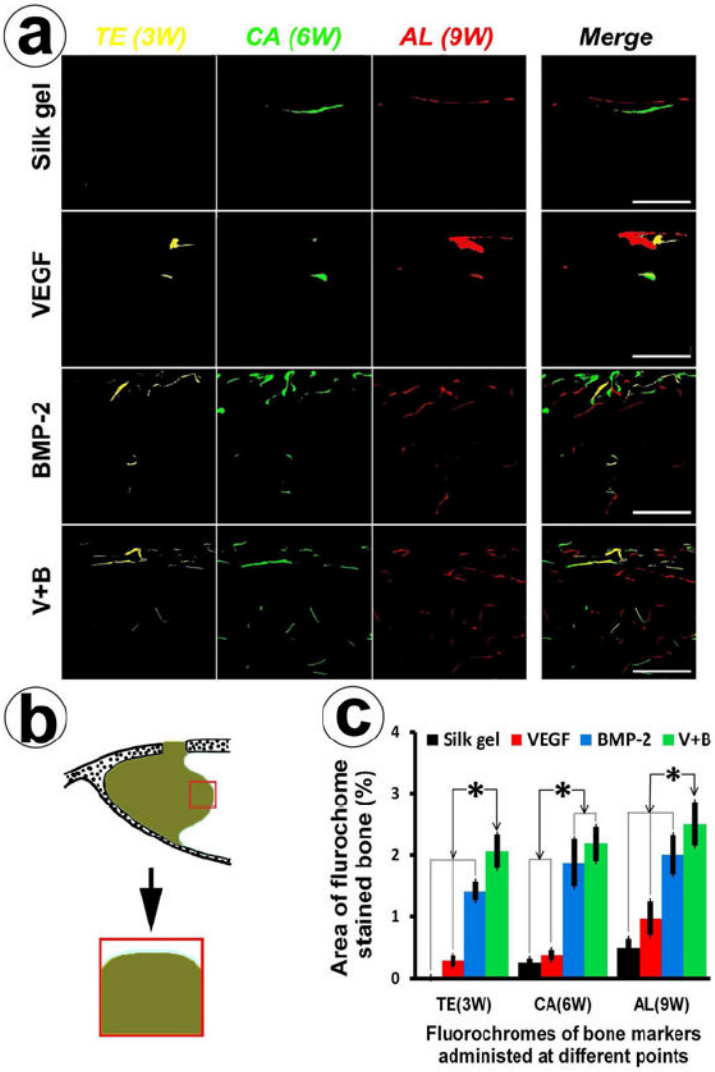

Fig. 4.

Sequential fluorescent labeling and histomophometric analysis. (a) Polychrome fluorescent labeling of TE, CA and AL was administrated at 3, 6, 9 weeks post-operation. Images of column “Merge 1” represent the merged three fluorochromes. “Merge 2” column represents merged images of the three fluorochromes together with the plain confocal laser microscope image (bar = 500 μm). (b) This scheme indicates the selected region used for quantifying the area of fluorochrome labeling (red color rectangle labeled region). (c) This graph represents the percentage of the labeled area of the three fluochromes of the four groups at different periods (* indicates significant differences, $p < 0.05$).

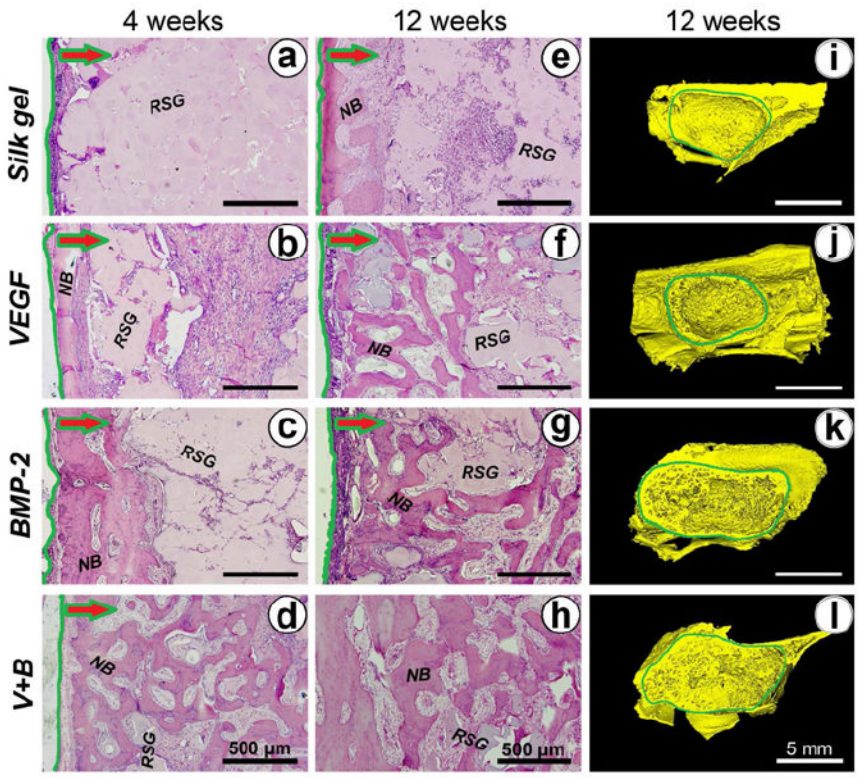

Fig. 5.

New bone formation detected by hematoxylin and eosin staining and Micro-CT. (a-d) and (e-h) shows local histological images of the different groups at 4 and 12 weeks post-operation, respectively. Green lines label the boundary of the augmented sinus region. The arrows indicate the direction of newly formed tissue ingrowth into the silk gel from the boundary. (NB: new bone; RSG: remnant silk gel). (i-l) Three dimensional reconstructed images of augmented sinus were taken 12 weeks after operation.

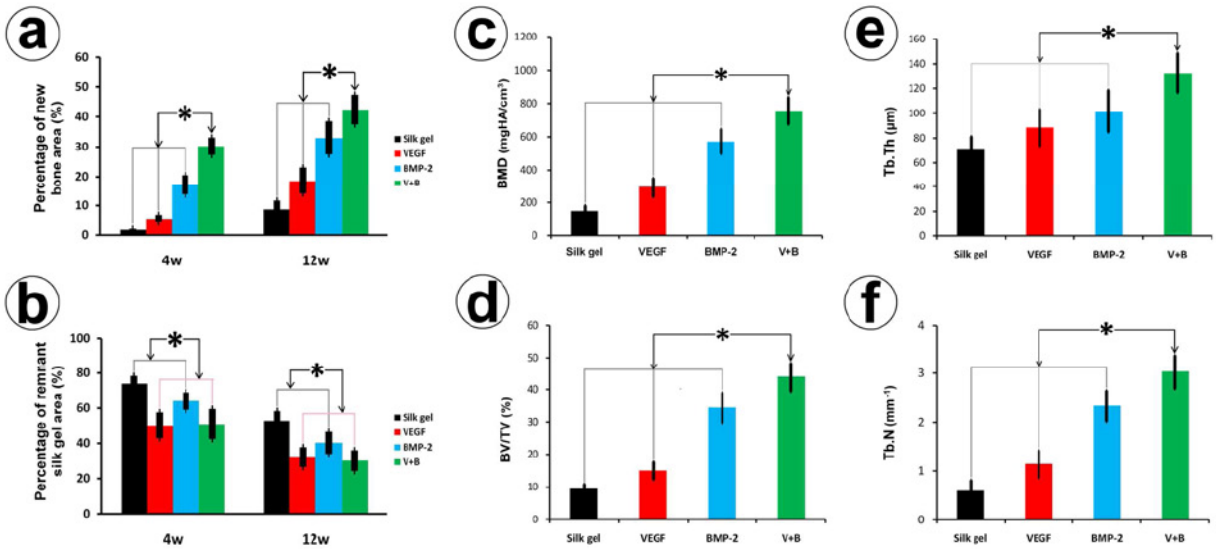

Fig. 6.

Histomorphometric analysis of the (a) bone formation and (b) remnant silk gel were also calculated for four groups at 4 and 12 weeks post-operation (* indicates significant differences, $p < 0.05$). The quantitative variables from Micro-CT scans of (c) Bone mineral density (BMD), (d) the ratio of bone volume to total volume (BV/TV), (e) trabecular thickness (Tb.Th) and (f) trabecular number (Tb.N) were calculated to assess the quality of newly formed bone in the different groups.

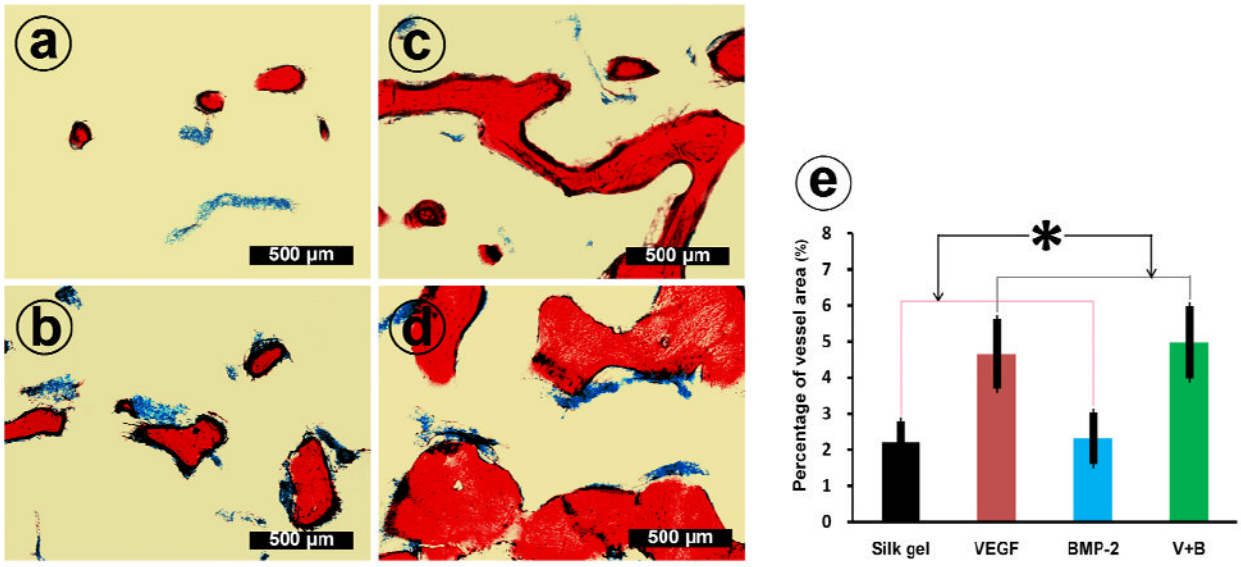

Fig. 7.

The undecalcified sections of group Silk gel (a), group VEGF (b), group BMP-2 (c) and group V+B (d) at 12 weeks post-operation were further stained with Von Gieson's picro fuchsin. On those nondecalcified sections, red areas represent newly formed bone and blue areas belong to blue colored Microfil which indicate newly formed blood vessels. (e) This graph shows the percentage of newly formed blood vessel area in the four groups (* indicates significant differences, $p < 0.05$).

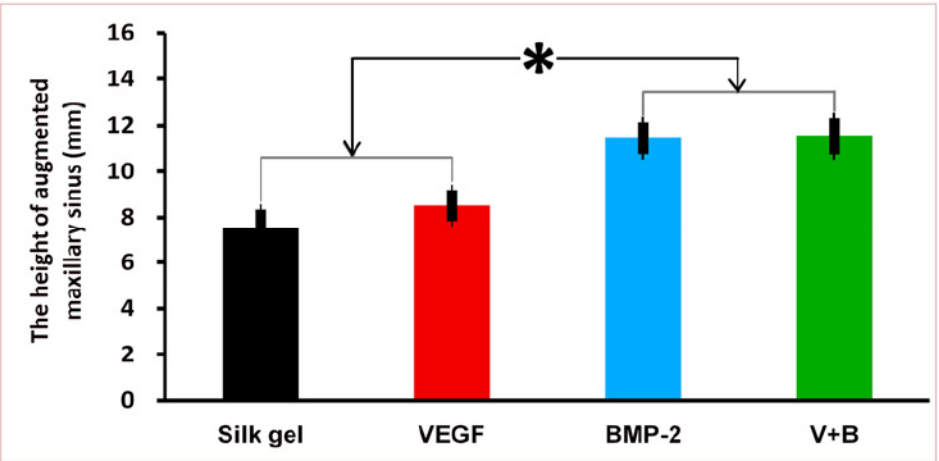

Fig. 8.

Augmented sinus height of the different groups at 12 weeks (* indicates significant differences, $p < 0.05$).

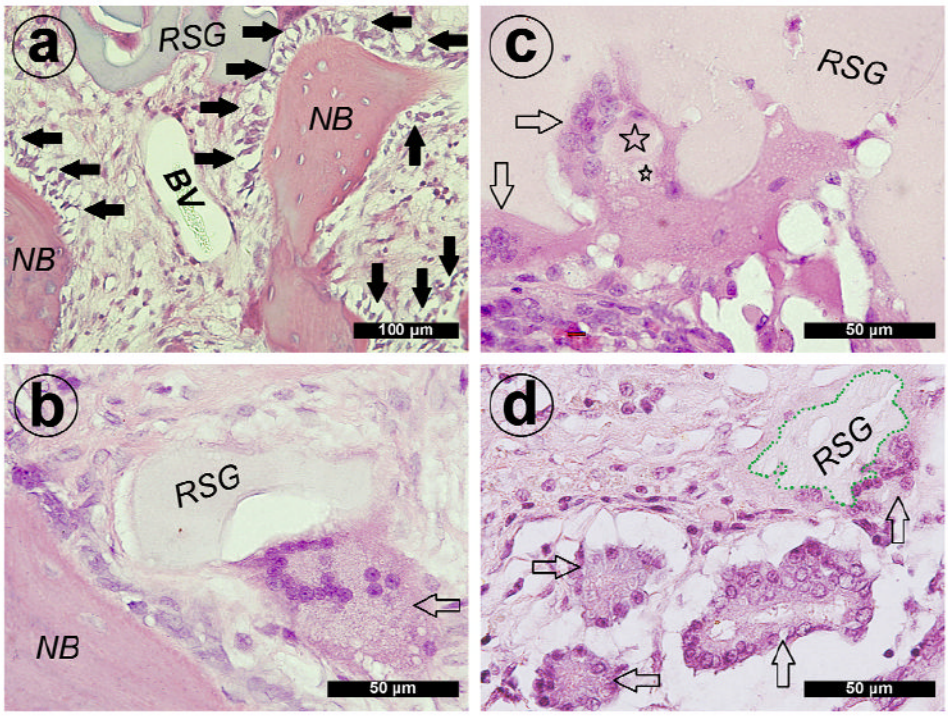

Fig. 9.

Hematoxylin and eosin staining of decalcified sections of group V+B. (a) New bone (NB) and blood vessel (BV) formation around remnants of the silk gel (RSG). A line of active osteogenic cells was observed around the newly formed bone (solid arrows show active osteogenic cells). At 4 weeks post-operation, (b) multinucleated giant cells quickly invaded into the silk gel and were observed around remnants of the silk gel (blank arrow shows multinucleated giant cell). (c) Silk gel fragments engulfed by the giant cells were also detected (☆ = small silk gel fragments). At 12 weeks post-operation, more giant cells invaded into the silk gel (the boundary of remnants of the silk gel marked with green dash line; blank arrow shows multinucleated giant cells).